Effects of NRF-1 and PGC-1α Cooperation on HIF-1α and Rat Cardiomyocyte Apoptosis Under Hypoxia

Nan Niu
School of Basic Medicine, Ningxia Medical University https://orcid.org/0000-0002-5123-6625
Hui Li
School of Basic Medicine, Ningxia Medical University
Xiancai Du
School of Basic Medicine, Ningxia Medical University
Chan Wang
School of Basic Medicine, Ningxia Medical University
Junliang Li
School of Basic Medicine, Ningxia Medical University
Jihui Yang
School of Basic Medicine, Ningxia Medical University
Cheng Liu
School of Basic Medicine, Ningxia Medical University
Songhao Yang
School of Basic Medicine, Ningxia Medical University
Yazhou Zhu
School of Basic Medicine, Ningxia Medical University
Wei Zhao (zw-6915@163.com)
School of Basic Medicine, Ningxia Medical University

Research

Keywords: NRF-1, apoptosis, cardiomyocytes, hypoxia, HIF-1α

Posted Date: February 10th, 2021

DOI: https://doi.org/10.21203/rs.3.rs-181724/v1

Abstract

Background: Hypoxia is a primary inducer of cardiomyocyte injury, its significant marker being hypoxia-induced cardiomyocyte apoptosis. Nuclear respiratory factor-1 (NRF-1) and hypoxia-inducible factor-1α (HIF-1α) are transcriptional regulatory elements implicated in multiple biological functions, including oxidative stress response. However, their roles in hypoxia-induced cardiomyocyte apoptosis remain unknown. The effect HIF-α, together with NRF-1, exerts on cardiomyocyte apoptosis also remains unclear.

Methods: We established a myocardial hypoxia model and investigated the effects of these proteins on the proliferation and apoptosis of rat cardiomyocytes (H9C2) under hypoxia. Further, we examined the association between NRF-1 and HIF-1α to improve the current understanding of NRF-1 anti-apoptotic mechanisms.

Results: The results show that NRF-1 and HIF-1α are important anti-apoptotic molecules in H9C2 cells under hypoxia, although their regulatory mechanisms differ. NRF-1 could bind to the promoter region of *Hif1a* and negatively regulate its expression. Additionally, HIF-1β exhibited competitive binding with NRF-1 and HIF-1α, demonstrating a synergism between NRF-1 and the peroxisome proliferator-activated receptor-gamma coactivator-1α.

Conclusion: These results indicate that cardiomyocytes can regulate different molecular patterns to tolerate hypoxia, providing a novel methodological framework for studying cardiomyocyte apoptosis under hypoxia.

Background

Hypoxia is characterized by insufficient blood supply resulting from various factors. It is the primary cause of cardiomyocyte injury [1, 2]. Apoptosis is one of the primary forms of myocardial cell death [3, 4], and hypoxia-induced apoptosis is a strong indicator of myocardial damage. In our previous study, the nuclear respiratory factor-1 (NRF-1) was found to alleviate the damage caused to myocardial cells by cobalt chloride, an anoxic chemical agent, by inhibiting apoptosis [5]. NRF-1 is a 68 kDa nuclear transcription regulator that was initially detected in a study on the activation and expression of cytochrome c [6]. It plays an important role in integrating the interaction between the nucleus and mitochondria, inducing mitochondrial gene expression, and regulating energy metabolism [7, 9]. Subsequent studies have been conducted on the structure and function of NRF-1 and oxidative respiration in mitochondria, which are closely associated with cell growth, immune response, apoptosis, embryonic development, and regulation of stress-responses in the endoplasmic reticulum [10–13]. However, limited research has been conducted on the effects of NRF-1 on cardiomyocyte apoptosis under hypoxia. While a study has shown that NRF-1 overexpression can increase cell sensitivity to apoptosis [11], while others have reported contradicting results; for instance, NRF-1 may activate mitochondrial biogenesis-related genes to achieve an anti-apoptotic effect [14]. Moreover, NRF-1 requires coactivators, such as peroxisome proliferator-activated receptor gamma coactivator 1-alpha (PGC-1α), for regulating

its target genes. NRF-1 transcription can be enhanced by binding to PGC-1α [15], which is a transcription factor capable of synergizing with other transcription factors to regulate gene expression, as well as other cellular physiological and metabolic reactions, such as mitochondrial biogenesis, apoptosis, and cell fate determination [16, 17]. Therefore, the regulatory effect of NRF-1 on cardiomyocyte apoptosis may be dependent on the co-participation of PGC-1α.

Hypoxic reactions are primarily characterized by a series of subsequent molecular events caused by reduced or completely depleted oxygen content. Hypoxia-inducible factors (HIFs) are a class of nuclear transcription regulatory factors closely related to physiological responses to hypoxia. They are divided into three subtypes, and each is composed of α and β subunits, namely HIF-1α and β, HIF-2α and β, and HIF-3α and β. The levels of HIFs increase steadily under hypoxia, and these proteins contribute to the cellular oxygen stress response [18, 20]. HIF-1 is presently one of the most widely studied molecules. Under normoxic conditions, proline residues on HIF-1α are hydroxylated by prolyl hydroxylase, which is recognized and ubiquitinated by E3 ubiquitin ligase, and rapidly degraded by proteasomes. However, under hypoxia, proline hydroxylase, which uses oxygen molecules as auxiliary matrices, is inhibited. This leads to the accumulation of HIF-1α in the cytoplasm, following which the protein enters the nucleus and combines with HIF-1β to form a dimer, which then regulates the expression of downstream genes [21]. Whole-genome chromatin immunoprecipitation (ChIP) analysis revealed that the promoter region of several genes possesses a HIF-1-binding element (5'-A/TCGTG-3', Hypoxia Response Element, HRE). This element can trigger various metabolic reactions, including those related to cell energy metabolism, vascular regeneration, cell proliferation, and immune and inflammatory reactions [22–24]. HIF-1α has also been shown to suppress apoptosis of rat brain cells during cerebral ischemia–reperfusion injury, by influencing B-cell lymphoma (BCL)-2 expression and participating in the regulation of p53 and the phosphatidylinositol 3 kinase/protein kinase B apoptotic pathway [25–28]. However, the mechanistic role of HIF-1 in hypoxia-induced cardiomyocyte apoptosis remains unclear. Additionally, the relationships between NRF-1 and HIF-1 under hypoxia, as well as the effect of NRF-1 on cardiomyocyte apoptosis, have not yet been characterized.

Since hypoxia-induced cardiomyocyte apoptosis accounts for one of the major risk factors for cardiac failure, preventing cardiomyocyte apoptosis under hypoxia is of particular importance. NRF-1 can alleviate cardiomyocyte apoptosis and enhance cell viability; however, the underlying mechanism remains elusive. Although several important associations between the HIF-1 dimer and hypoxia stress and apoptosis have been documented, a gap of knowledge regarding cardiomyocyte apoptosis under hypoxia persists. Whether a regulatory interaction between NRF-1 and HIF-1α exists and potentially affects the occurrence of cardiomyocyte apoptosis warrants further research. This study examines the effect of NRF-1 on cardiomyocyte apoptosis by establishing a hypoxia model of cardiomyocytes, to study the interaction between NRF-1 and HIF-1α individually and in relation to apoptosis under hypoxia. Our objective is to provide new therapeutic alternatives and a theoretical basis for the treatment and intervention of heart failure.

Methods

Cell culture

H9C2 and 293T cells were purchased from the Chinese Academy of Sciences (Shanghai, China); 293T cells were used to package lentivirus, while H9C2 was employed to construct cell lines and in related experimental studies. The plasmids used in this study were used to transform *Escherichia coli* cells, followed by amplification, clonal selection, enzyme digestion, sequencing, and further amplification to obtain the required plasmids.

Construction of lentivirus-transfected cardiomyocytes

All transfection reagents were obtained from PolyJet™ (Signagen Company, Jinan City, China). Further, 293T cells were subcultured in a 10-cm culture dish; when they reached 80–90% confluence, the original medium was discarded, and 5 mL of fresh Dulbecco's modified Eagle's medium (DMEM, Gibco Company, New York, USA) supplemented with 10% fetal bovine serum (FBS, Gibco Company, New York, USA) was added. Cells were subsequently incubated for 30–60 min. For each 10-cm cell culture dish, plasmid suspension was prepared in 500 μL serum-free DMEM in a 1:1 ratio of packaging plasmid to lentiviral expression plasmid, i.e., pLP1:pLP2:pLPVSVG:pCDH-CMV/pGreenPuro/sh-NRF1/sh-HIF1α at a ratio of 1:1:1:1 (6 μg: 6 μg: 6 μg: 6 μg) and subjected to vortex oscillation. Next, 500 μL of serum-free DMEM was mixed with 60 μL of PolyJet™ transfection reagent. After mixing gently, the medium containing PolyJet™ transfection reagent was added to the plasmid mixture, which was then allowed to stand for 15 min at room temperature (20°C). After 48 h, the virus particles were collected by centrifugation at 4°C, 50,000 × *g* for 2 h (ultrahigh-speed). Next, 1×10^6 H9C2 cells were seeded on a six-well plate. Once cells adhered, the supernatant was discarded, and 2 mL of lentiviral transfection suspension containing 2% FBS and 8 μg μL^{-1} polybrene (Sigma Aldrich, Germany) was added. After 72 h, the fluorescence intensity was measured. The cells were screened after being treated with 1 mg mL^{-1} puromycin (Sigma Aldrich, Germany) for 2 weeks. After another week of culture, the stably transfected cells were screened using an ARIA III flow cytometer (BD Company, New Jersey, USA). The empty vector cardiomyocytes were named pCDH-CMV and pGreenPuro, the NRF-1 overexpression cardiomyocytes were named pCDH-NRF1, the NRF-1-inhibited cardiomyocytes were named sh-NRF1, and the HIF-1α-inhibited cardiomyocytes were named sh-HIF1α.

Establishment of the hypoxia model

The cells were subcultured in three T-75 cm^2 cell culture bottles, and the experiment was initiated when the cells reached 90% confluence. A day before hypoxia induction, 1×10^7 cells were subcultured in a 10-cm culture dish and placed in the incubator at 37 ℃ overnight to be used when needed. On the second day under anoxia, the medium was removed to the maximum extent possible. Next, 10 mL of cell culture medium was added to each dish. The dishes were placed in a three-gas incubator, and the timer was set to start when the oxygen concentration reached 1%. After completion, the nitrogen valve in the anoxic concentration detection table was used to reduce the oxygen

concentration to 1%. After treatment under hypoxia, the cells were rapidly placed in the anoxic operation table to extract total protein or RNA.

Western blotting

The primary components of the pyrolysis solution were as follows: 50 mM Tris-HCl (Sigma Aldrich, Germany), 150 mM NaCl (Sigma Aldrich, Germany), 1% Triton X-100 (Sigma Aldrich, Germany), 1% sodium deoxycholate (Sigma Aldrich, Germany), 0.1% SDS (Sigma Aldrich, Germany), and 5 mM EDTA (Sigma Aldrich, Germany). Along with this, 200 μg μL^{-1} aprotinin (Sigma Aldrich, Germany), 1 μg μL^{-1} leupeptin (Sigma Aldrich, Germany), 1 mM PMSF (Solarbio Life Science, Beijing, China), 10 mM $MgCl_2$ (Thermo Fisher Scientific, Waltham, MA, USA), and 40 U benzonase nuclease (Haigen Biotech, Sanghai, China) were added. All processes were performed on ice. To each 10-cm culture dish, 1 mL of the prepared lysate was added. The cells were scraped and added to a microcentrifuge tube and maintained for 15 min, shaken for 10 s every 5 min, and centrifuged at 12,000 × *g* for 15 min. The supernatant was then collected. Next, 100 μL of the supernatant was mixed with 25 μL of protein loading buffer and boiled at 100°C for 10 min. This was followed by western blotting. After total protein extraction, 20 μL of protein was loaded. The conditions for electrophoresis were as follows: 120 V for 15 min, and 150 V for 55 min. After electrophoresis, the proteins were transferred to a polyvinylidene fluoride (PVDF, Sigma Aldrich, Germany) membrane under a constant current (300 mA) for 2 h. The PVDF membrane was placed in a buffer solution containing PBS (Solarbio Life Science, Beijing, China) + 0.05% Tween 20 (Solarbio Life Science, Beijing, China) and sealed for 4 h. The antibody dilutions used were as follows: DNA methyltransferase (DNMT)-1 (24206-1-AP, 1:1,000; Protech, Rosemont, USA), HIF-1α (NB100-105, 1:1,000; Novus Biologicals, Briarwood, USA), HIF-1β (NB100-124, 1:1,000; Novus Biologicals, Briarwood, USA), PGC-1α (NBP1-04676, 1:1,000; Novus Biologicals, Briarwood, USA), NRF-1 (ab175932, 1:2,000; Abcam, Cambridge, England), β-actin (ab49900, 1:10,000, HRP-conjugated; Abcam, Cambridge, England), BCL-2 (sc-7382, 1:500; Santa Cruz Biotechnology Inc., Texas, USA), BCL-2-associated X protein (Bax; ab32503, 1:2,000; Abcam, Cambridge, England), and BCL-extra-large (BCL-xL; ab32370, 1:1,000; Abcam, Cambridge, England). The proteins were treated with the primary antibody overnight at 4°C. This was followed by treatment with goat anti-rabbit (Bioss Antibodies, Beijing, China) and goat anti-mouse (Bioss Antibodies, Beijing, China) secondary antibodies (1:25,000) for 4 h. After washing the membrane with PBST, the protein levels were measured using a ChemiDoc MP Imaging System (Bio-Rad Laboratories, Hercules, CA, USA). Image Lab 5.1 (Bio-Red, California, USA) was used to analyze gray values.

Immunoprecipitation

The steps for lysate preparation and total protein extraction were the same as those described for western blotting. For western blotting, 100 μL of protein was used, and the remaining protein supernatant was used for immunoprecipitation. The samples were stored in ice until further use. Each 900 μL protein lysate sample was mixed with 1 μg of immunoprecipitation antibodies and placed on the microcentrifuge tube rack of a rotary mixer. The instrument was placed in a refrigerator at 4°C overnight. The next day, 1 μL of pre-mixed magnetic beads (Thermo Fisher Scientific, Waltham, MA, USA) were added to the sample, in a refrigerator at 4°C for 1 h. The liquid was then discarded,

and 900 μL of pre-cooled lysis buffer containing a protease inhibitor was added, followed by gentle mixing and washing thrice. Next, 50 μL 1× protein loading buffer (Solarbio Life Science, Beijing, China) was added, and the sample was mixed well, boiled at 100°C for 10 min, incubated on ice, and stored. The subsequent steps were the same as those described for western blotting.

ChIP assay

The cells were spread on 10-cm Petri dishes with a convergence degree of approximately 90%. To every culture dish, 10 mL of DMEM and 275 μL of fresh 37% formaldehyde (Sigma Aldrich, Germany) were added, and cross-linking was allowed for 10 min. Next, 10× glycine was added to quench excess formaldehyde, and the suspension was mixed and incubated for 5 min. The residual medium was discarded, 10 mL of pre-cooled PBS was added, and the cells were washed. To the culture dish, 1 mL of pre-cooled PBS containing a protease inhibitor was added. The cells were then scraped into a microcentrifuge tube and centrifuged at 700 × *g* at 4°C for 3 min. The supernatant was discarded, and the cells were resuspended in SDS lysis buffer containing a protease inhibitor. The cells were incubated on ice before ultrasonication (Xinzhi Biotechnology Co., Ltd, Ningbo, China). The ultrasonication conditions were as follows: power, 50 W, ultrasonication for 5 s, stop for 55 s, repeated eight times. Next, protein-G agarose beads (Thermo Fisher, Norway) were added to the ultrasonicated products, followed by mixing for 1 h on the rotary mixer at 4°C. The supernatant was collected by centrifugation and distributed into two microcentrifuge tubes. Next, 1 μg of normal rat IgG (Sangon Biotech, Shanghai, China) and 1 μg of antibody were added to the two tubes, and the mixture was incubated overnight at 4°C. The next day, agarose beads were added to trap the protein–DNA complexes, followed by washing, elution of the protein–DNA complexes using an eluent buffer, and purification of DNA after cross-linking. Primers sequences for Hif1a promoter region used in this study are listed in Table 1.

Table 1
Primer sequences for *Hif1a* promoter region

Bases upstream of *Hif1a* promoter	Primer sequence (5'–3')	Size (bp)
-1922 to -1511	F: ATCGCCCTATGTGGTTTC	412
	R: AAGGTCCTGGCTTCAAAA	
-1331 to -1135	F: CATTATTATACAACCCAACG	197
	R: CAAGCCCAACAAAGGAAC	
-1147 to -1020	F: TTTGTTGGGCTTGGAATA	128
	R: TGTGCTGGGAACTATGGA	
-997 to -815	F: GTCTGTAGGTTGGAGGATG	183
	R: GAGTGACAAGGCAGGAAA	
-641 to -455	F: TAATGACTTGGAGACTTCCCTT	187
	R: TCCTTAGTTGCGTGGTTG	
-472 to -200	F: CAACCACGCAACTAAGGA	273
	R: AATCAGGAGGAGGTCAGC	
-199 to -19	F: AGAGCAACGTGGGCTGGGGTGG	146
	R: AGGGGAGGGGAGCAAAGG	
-447 to -113	F: CCAACCACGCAACTAAGGA	334
	R: AGAGCCAATGGGAAAGGAC	
-447 — +136	F: CCAACCACGCAACTAAGGA	583
	R: TTGCTCCTCCGGCTGGCTTGTC	
-191 to + 136	F: GCTGACCTCCTCCTGATTG	327
	R: TTGCTCCTCCGGCTGGCTTG	
-191 to + 374	F: GCTGACCTCCTCCTGATTGG	565
	R: CGGCCCGGCTTACTTT	

Polymerase chain reaction (PCR)

DNA obtained using a DNA extraction kit (Omega Biotek, Inc., Norcross, GA, USA) or purified DNA from the ChIP assay was used as the template. The primer sequences are listed in Supplementary Table S1. The reaction system and related reagents are listed in Supplementary Table S2. The reaction conditions were

as follows: pre-denaturation at 95°C for 2 min; 30 cycles of denaturation at 95°C for 15 s, annealing at 55–65°C for 15 s, extension at 68°C for 10 s; and preservation at 4°C. The samples were separated by electrophoresis using a 0.5% agarose gel.

RNA extraction

RNA was extracted using TRIzol reagent (Thermo Fisher Scientific, Waltham, MA, USA). Briefly, 2–5 × 10^6 cells were subcultured in six-well plates. TRIzol reagent (1 mL) was added into each well, and the suspension was distributed in enzyme-free microcentrifuge tubes. Next, 200 μL chloroform (Sigma Aldrich, Germany) was added; the mixture was shaken for 15 s, incubated on ice for 15 min, and centrifuged at 12,000 × *g* for 15 min; and the supernatant was collected. An equal volume of isopropanol was added, and the solution was mixed well, incubated on ice for 10 min, and centrifuged at 12,000 × *g* for 10 min. Further, the supernatant was discarded, 75% ethanol was added, and the solution was centrifuged at 7,500 × *g* for 5 min. After air-drying, 50 μL of enzyme-free ddH_2O was added to dissolve RNA, and the samples were stored at − 80°C for subsequent experiments.

Reverse transcription

A cDNA Reverse Transcription Kit (Thermo Fisher Scientific, Waltham, MA, USA) was used for the reverse transcription experiment. The reaction system is outlined in Supplementary Table S3.

Real-time qPCR

The qPCR reagent was purchased from DBI Bioscience (Ludwigshafen, Germany). After preparing the reaction system, a real-time PCR amplification instrument (StepOne™ Real-Time PCR System, Thermo Fisher Scientific, Waltham, MA, USA) was used for performing PCR. The reaction conditions were as follows: pre-denaturation at 95°C for 2 min; denaturation at 95°C for 15 s, annealing at 60°C for 30 s, cycling at 72°C for 30 s; generation of dissolution curve, cycling at 95°C for 15 s, annealing at 60°C for 30 s, and cycling at 72°C for 30 s. The template quality and primer specificity were determined from the dissolution and amplification curves. The target gene mRNA levels were calculated using the $2^{-\triangle\triangle CT}$ method; rat β-actin was used as an internal reference control. The reaction system and primer sequences are listed in Supplementary Table S4 and Supplementary Table S5, respectively.

Real-time evaluation of cell proliferation

Before evaluating cell proliferation, the cells were counted, and the concentration was adjusted to 15 × 10^5 cells per mL per well. Real-time cell analysis (ACEA Biosciences, California, USA) was used. The detection time was adjusted to measure the cell proliferation level every 10 min, and the detection duration was 24–48 h. The cells in each well were labeled, and 150 μL of complete medium was added into the special plate (8-well) to deduct the base value. Next, 300 μL of cell suspension was added into each well, and the cell state was assessed microscopically (EVOS™ XL Core Imaging System, Thermo Fisher, Waltham, MA, USA). After evenly spreading out the suspension, the plates were placed on an ultra-clean workbench for 30 min and then transferred to the instrument, with the entire detector placed in the

e cells were observed. For hypoxic cultures, after overnight

adherence, the entire instrument was placed in the three-gas incubator, and cells were observed after the oxygen concentration was adjusted to 1%.

Evaluation of caspase-3 activity

For this experiment, 5–10 × 10^6 cells were seeded on a 10-cm cell culture dish 1 day in advance. The next day, 10 μL of DTT was added per mL of lysis buffer and detection buffer. After hypoxic or normal culturing, the medium was discarded, and 500 μL of the aforementioned cold cell lysate was added. The cells were scraped into a microcentrifuge tube, mixed by vibration at high speed for 15 s, placed on ice for 15 min with shaking for 15 s every 5 min, and centrifuged at 12,000 × *g* for 15 min. The supernatant was collected into a fresh tube, and the protein levels were quantified using the Bradford assay. A 96-well plate was prepared for each group, and three repeat wells were assigned. Next, 10 μL of protein supernatant (containing 30–50 μg of total protein) was collected from each well, the lysate was added, and the suspension was mixed well. Following this, 10 μL of Ac-DEVD-pNA (BestBio, Nanjing, China) was added, and the culture was incubated in the dark at 37°C for 4 h until the solution turned yellow. Detection was performed by measuring absorbance at 405 nm. Caspase-3 activity was measured based on the ratio of the treated group absorbance to that of the blank control group.

Real-time observation of cell apoptosis

The experiment was performed in a Biotek Cytation 5 (BioTek, Vermont, USA). Briefly, the plate bottom height was adjusted, the six-well plate mode was selected, and 1 × 10^6 cells were seeded in the six-well plate. After overnight adherence at 37°C, the plate was placed on a test bench. The focus, exposure time, channel, and other parameters were adjusted, and red and blue fluorescence were detected simultaneously for each well, once every 10 min. The temperature was set at 37°C, and the oxygen concentration was fixed at 1%. Automatic imaging and videography were performed. The cell proliferation curve was generated using the Gen5 software (BioTek, Vermont, USA).

Bisulfite sequencing PCR

DNA was extracted according to the method described in the PCR section. Based on the sequence predicted by the MethPrimer tool [29–31], primers were designed for DNA extraction. Details of the reaction system and primer sequences are outlined in Supplementary Table S6 and Supplementary Table S7, respectively. The reaction conditions were as follows: Pre-denaturation at 95°C for 5 min; 35 cycles of denaturation at 95°C for 30 s, annealing at 55–60°C for 30 s, and extension at 72°C for 45 s; and extension for 10 min at 72°C. The sequencing process was commissioned to Sangon Biotech (Shanghai, China).

The gene sequence is as follows (5– 3):

GAGAGCAACGTGGGCTGGGGTGGGGCCTGGCCGCCTGCGTCCTTTCCCATT
GGCTCTCGGGGAACCCGCCTCCGCTCAGGTGAGGCGGGCCCGCGGGTGCGCGC
GTCGGGCTTAGCGGGCGCGCGCAGCCCTTTGCTCCCCTCCCCTCGCCGCGCGC
CCGAGCGCGCCTCCGCCCTTGCCCGCCCCCTGCCGCTGCCTCAGCGCCTCAGTG
CACAGAGG

After bisulfite treatment, the cytosine residues were changed to thymine, with the CG sites retained as "C," as shown in the following (5– 3):

GAGAGTAACGTGGGTTGGGGTGGGGTTTGGTCGTTTGCGTTTTTTTTTATTG
GTTTTCGGGGAATTCGTTTTCGTTTAGGTGAGGCGGGTTCGCGGGTGCGCGCGT
CGGGTTTAGCGGGCGCGCGTAGTTTTTTGTTTTTTTTTTTTCGTCGCGCGTTCGA
GCGCGTTTTCGTTTTTGTTCGTTTTTTGTCGTTGTTTTAGCGTTTTAGTGTATAGA
GG

Statistical analysis

SPSS 17.0 (IBM Corporation, New York, USA) was used for statistical analysis. The results were expressed as mean ± standard deviation, and $P < 0.05$ was considered statistically significant. Student's *t*-test was used to compare the means of two samples. One-way analysis of variance was used for comparing multiple samples. Student–Newman–Keuls test was used for pairwise comparison between groups, with $P < 0.05$ representing statistically significant differences.

Results

NRF-1 affects cardiomyocyte apoptosis

For a preliminary investigation of the effect of NRF-1 on cardiomyocyte apoptosis under hypoxia, we used H9C2 cells as the target cells at 1% oxygen concentration. First, we developed an NRF-1-overexpressing cardiomyocyte cell line (pCDH-NRF1) and an NRF-1-inhibited cardiomyocyte cell line (sh-NRF1; Fig. S1, Fig. S2, and Table S1) and studied the proliferation levels of these cells. The results showed that under normoxia (21% O_2 + 5% CO_2 + 74% N_2), NRF-1 could promote cell proliferation; however, when NRF-1 expression was inhibited, cardiomyocyte proliferation decreased. Under hypoxia (1% O_2 + 5% CO_2 + 94% N_2), cardiomyocyte proliferation was restricted in all groups; subsequently, NRF-1 overexpression significantly alleviated the decline in cell proliferation. In addition, the inhibition of NRF-1 aggravated the hypoxia-induced suppression of cell proliferation (Fig. 1A, B). These results indicate the [illegible]ed cardiomyocyte injury. To further verify whether the

protective effect of NRF-1 is mediated by its anti-apoptotic effect, the different levels of cardiomyocyte apoptosis were evaluated. Caspase-3 is crucial for the execution of apoptosis. Activated caspase-3 can cleave DNA or induce its degradation to RNA; inhibit cytoskeletal protein synthesis; and ultimately induce nuclear pyknosis, fragmentation, and cell membrane disintegration [32, 33]. These results substantiated that under hypoxia, the activity of caspase-3 increased gradually, and NRF-1 could suppress this increase (Fig. 2A). Furthermore, with the prolongation of hypoxia time and the activation of caspase 3 the state of myocardial cells in each group gradually deteriorated, and the cells began to disintegrate and undergo pyknosis and nuclear fragmentation. Cell membrane integrity is lost during cell apoptosis, and propidium iodide can enter the damaged nucleus and stain the DNA. Apoptotic and necrotic cells showed bright red fluorescence, with peak fluorescence at approximately 6 h; however, NRF-1 delayed this process to approximately 10 h (Fig. S3). Subsequently, the expression of the apoptosis regulatory molecules BCL-2, BCL-xL, and Bax was compared. Our results showed that with an increase in hypoxia, the expression of NRF-1 and the anti-apoptotic proteins BCL-2 and BCL-xL decreased, whereas the expression of the pro-apoptotic protein Bax marginally increased. However, NRF-1 promoted the expression of BCL-2/BCL-xL and inhibited Bax expression (Fig. 2B, C). These results suggest that in hypoxia-induced myocardiocyte injury, NRF-1 offers protection from apoptosis.

NRF-1 can bind to the promoter region of *Hif1a* and inhibit its expression

It has been reported that in 293T cells, NRF-1 binds to the promoter region of *Hif-1α* and negatively regulates its expression [34]. The regulatory effects of NRF-1 on HIF-1α were therefore investigated. The primers were designed from the sequence of the rat *Hif1a* promoter region available on the Ensembl genome browser (https://asia.ensembl.org/index.html). After evaluating each primer annealing temperature, ChIP was performed to confirm the NRF-1 binding site in the promoter region of *Hif-1α*. Our data showed that the promoter region between − 1992 – -1511 and − 1147 – -455 upstream of *Hif1a* represented the NRF-1 binding site (Fig. 3A). To better elucidate the effect of NRF-1 on the binding site, qPCR was performed. It was observed that HIF-1α expression decreased significantly with the increase in NRF-1 expression (Fig. 3B). Similar results were obtained in the western blotting experiment, wherein the HIF-1α protein levels increased gradually with the prolongation of the duration of hypoxia; however, its expression could be inhibited by NRF-1 (Fig. 3C). The above data suggest that the binding of NRF-1 to the promoter region of *Hif1a* can inhibit its expression.

In addition, NRF-1 has been reported to activate the promoter region of *Dnmt-1*, influence its expression, regulate methylation levels, and further influence the expression of other genes [34, 35]. Since NRF-1 can inhibit the expression of HIF-1α at the transcriptional level, we attempted to determine whether NRF-1 regulates *Hif1a* expression by affecting its methylation. First, the PROMO online analysis tool (http://alggen.lsi.upc.es/cgi-bin/promo_v3/promo/promoinit.cgi?dirDB=TF_8.3) was used to predict whether NRF-1 has binding sites in the *Dnmt1* promoter region. Since PROMO does not have a rat

referred for the binding sequence and was compared to the

rat *Dnmt1* promoter sequence to identify the corresponding sequence. The data showed that NRF-1 had two binding sites in the promoter region of human *DNMT1*, and upon comparison with the promoter region sequence of rat *Dnmt1*, two similar sequences were obtained, which suggested that the binding sequence is conserved. Subsequently, primers for the sequence were designed (Fig. S4 A, B). After optimizing the annealing temperature, the ChIP assay was performed and revealed that NRF-1 could bind to the sequence (Fig. S4C). Next, the effect of NRF-1 overexpression on the DNMT-1 protein level was evaluated using western blotting. The results indicate that under hypoxia (for 0, 1, 2, 3, 6, 12, and 24 h), *Dnmt1* expression gradually decreased; however, it significantly increased following NRF-1 overexpression (Fig. S4D). Hence, it was next determined whether NRF-1 modulates HIF-1α expression by regulating its methylation through DNMT-1, leading to subsequent regulation of *Hif1a* transcription. Based on the information provided on the MethPrimer website (https://www.urogene.org/methprimer/), it was concluded that a CpG island was present in the promoter region of *Hif1a*. The methylation status of the *Hif1a* promoter before and after hypoxia was compared. The bisulfite sequencing PCR results revealed no significant change in the methylation status of the predicted sequences (Fig. S4E, F). Therefore, even though NRF-1 can regulate DNMT-1 expression, the regulation process does not affect HIF-1α, and NRF-1 directly inhibits HIF-1α.

HIF-1α inhibition by NRF-1 affects cardiomyocyte apoptosis

To evaluate the effect of HIF-1α inhibition by NRF-1 on cardiomyocyte apoptosis, the simultaneous inhibition of HIF-1α and NRF-1 under artificial conditions was performed. Preliminary experiments showed that hypoxia for 1 and 2 h did not induce an obvious oxygen stress response. Accordingly, hypoxia duration was set at 0, 3, 6, 12, and 24 h. Our data showed that HIF-1α suppression exacerbated the decline in cell proliferation induced by hypoxia and promoted caspase-3 activity; however, contrary to our expectation, NRF-1 expression increased, and the levels of the anti-apoptotic proteins BCL-2 and BCL-xL increased as well. These results indicate that similar to NIF-1, HIF-1α acts as an anti-apoptotic protein; furthermore, a mutually inhibitory relationship might exist between NRF-1 and HIF-1α, and the increase in BCL-2 and BCL-xL levels could result from the increase in NRF-1 expression caused by HIF-1α inhibition. To further evaluate the possibilities, HIF-1α and NRF-1 expression was inhibited. Compared with HIF-1α inhibition (sh-HIF1α), under hypoxia, the dual inhibition of NRF-1 and HIF-1α relieved the decline in cell proliferation and lowered caspase-3 activity. Unexpectedly, with the reduction in NRF-1 expression, the levels of BCL-2 and BCL-xL decreased, whereas the levels of HIF-1α increased (Fig. 4A, B, C). The above results reflect that although NRF-1 primarily regulates the expression of BCL-2 and BCL-xL, this is not the only mechanism that modulates apoptosis. Therefore, while HIF-1α can regulate apoptosis under hypoxia, it may do so in a BCL-2/BCL-xL-independent manner.

NRF-1 can compete with HIF-1α to bind to HIF-1β

Previous results suggested that HIF-1α might exert the same anti-apoptotic effect as NRF-1. Concurrently, the results also showed that NRF-1 and HIF-1α exhibited mutual expression inhibition. Furthermore, the effect exerted by this mutual inhibition was analyzed. HIF-1α has been shown to form a dimer with HIF-1β and thereby form a heterodimeric biological functions. This led us to investigate whether NRF-1

and HIF-1β interact, and if this affects other molecular events. Furthermore, the effect of this interaction on the binding of HIF-1α and HIF-1β warranted investigation. First, the binding among HIF-1α, NRF-1, and HIF-1β following NRF-1 interference (sh-NRF1) was evaluated. The results showed that similar to HIF-1α, NRF-1 could bind to HIF-1β. Further analysis showed that the level of NRF-1 and HIF-1β binding gradually decreased with the prolongation of hypoxia. Compared with the empty vector group (pGreenPuro), the NRF-1 inhibition group (sh-NRF1) showed a decrease in the level of NRF-1 and HIF-1β binding, and simultaneously, the level of HIF-1α and HIF-1β binding increased (Fig. 5A). These results indicated that a competitive binding interaction might exist between NRF-1 and HIF-1α for HIF-1β under hypoxia.

In this experiment, the effect of NRF-1 inhibition on the binding of HIF-1α to HIF-1β was studied. To effectively confirm the binding effect, dimethyloxallyl glycine (DMOG) and BAY 87-2243 (HY-15836, BAY 87-2243, MedChemExpress, New Jersey, USA) were used to treat the cells. DMOG stabilizes HIF-1α expression and enhances its cytoplasmic accumulation by inhibiting HIF prolyl hydroxylase [36, 37]. BAY 87-2243 is a highly effective selective inhibitor of HIF-1α expression. Neither of the two drugs affects HIF-1β expression. The immunoblotting experiment showed that DMOG could enhance HIF-1α expression in a dose-dependent manner, and with the increase in DMOG concentration, NRF-1 expression gradually decreased. However, this did not affect HIF-1β expression. In addition, the immunoprecipitation experiment showed that DMOG increased the levels of HIF-1α and HIF-1β binding, whereas it decreased the levels of NRF-1 and HIF-1β binding. Next, HIF-1α was suppressed to study the interaction between NRF-1 and HIF-1α under hypoxia. The results showed that BAY 87-2243 could effectively inhibit the increase in HIF-1α expression induced by hypoxia, and consistent with the previous finding, NRF-1 expression increased with HIF-1α inhibition and following the inhibition of HIF-1α by BAY 87-2243, the levels of NRF-1 and HIF-1β binding increased (Fig. 5B, C). These findings further confirmed the competitive binding between NRF-1 and HIF-1α.

PGC-1α participates in the competitive binding of NRF-1 and HIF-1α with HIF-1β

The regulatory effect of NRF-1 on cells is inseparable from the synergistic effect of PGC-1α. The role of PGC-1α was thus investigated. The results showed that PGC-1α expression decreased gradually with an increase in hypoxia duration, whereas NRF-1 inhibition did not alter PGC-1α expression. Findings from the immunoprecipitation experiment confirmed that PGC-1α and NRF-1 exhibited a stable binding relationship that did not change with hypoxia duration. The effect of this binding relationship on HIF-1α was evaluated. The results showed that DMOG could inhibit PGC-1α, and PGC-1α could combine with HIF-1β; however, the binding levels of PGC-1α reduced as in the case of NRF-1, with an increase in the concentration of DMOG and the accumulation of HIF-1α. Subsequently, the cells were treated with ZLN005 (HY-17538; MedChemExpress, New Jersey, USA), a drug that activates the transcription and expression of PGC-1α. This demonstrated that for different durations of hypoxia (0, 6, 12, and 24 h), PGC-1α intervention led to an increase in NRF-1 expression and a decrease in HIF-1α expression; however, this did not affect the expression of HIF-1β. Yet, the increase in PGC-1α expression induced by ZLN005 enhanced the binding between NRF-1 and HIF-1β and suppressed the binding between HIF-1α and HIF-1β

(Fig. 6A, B, C). The above results indicate a novel binding mechanism among NRF-1/PGC-1α, HIF-1α, and HIF-1β.

Discussion

Apoptosis accompanies myocardiocyte injury induced by ischemia and hypoxia [38]. Cardiomyocyte apoptosis is common to almost all types of heart diseases [38–42]. To alleviate the effect or avoid the occurrence of cardiomyocyte apoptosis, especially the extensive damage caused by cardiomyocyte apoptosis under hypoxia injury, extensive studies were conducted. Cobalt chloride was used to simulate hypoxia in cardiomyocytes at an early stage, and NRF-1 expression was detected in cardiomyocytes. NRF-1 overexpression was found to alleviate cardiomyocyte apoptosis induced by chemical hypoxia. To further investigate effects of NRF-1 on cardiomyocyte apoptosis, especially under actual hypoxic conditions, we used three-gas incubators to reduce the oxygen concentration to 1%. The results showed that the overexpression and inhibition of NRF-1 could affect cell growth and proliferation under normoxic conditions. While NRF-1 overexpression promoted cell growth, its inhibition suppressed cell proliferation. These results indicate that NRF-1 can promote cell proliferation, and NRF-1 inhibition affects cell division and growth, similar to the finding that NRF-1 knockout is lethal in mouse embryos [43]. This result established that NRF-1 plays an important role in the cell viability and growth of individual organisms. Subsequently, we studied the effect of NRF-1 on cardiomyocyte proliferation under different durations of hypoxia. The results showed that in the first few hours (6 h) under hypoxia, the cells maintained a certain proliferation level. This observation may be attributed to the residual oxygen in the solution. However, as oxygen was progressively depleted with the increase in hypoxia duration, cardiomyocyte proliferation decreased in each group. Notably, the overexpression of NRF-1 significantly slowed the decline in cell proliferation, whereas the cell proliferation level decreased significantly upon NRF-1 inhibition. These results indicate that NRF-1 can protect cardiomyocytes from hypoxia and highlight the anti-apoptotic mechanism adopted by NRF-1.

The decrease in cell proliferation under hypoxia may be caused by cell necrosis, apoptosis, and autophagy. To further dissect the role of apoptosis in hypoxia, we observed the level of apoptosis-related molecules. As mentioned above, caspase-3 is the primary executor of apoptosis. In transgenic mice, caspase-3 overexpression increased the infarct size of cardiomyocytes caused by oxygen stress and increased the likelihood of death in mice [44]. Conversely, the downregulation of caspase-3 reduced the apoptotic index and improved cardiac function after myocardial infarction [45, 46]. We first assessed the activity of caspase-3 in different groups of cardiomyocytes under hypoxia to observe whether the decrease in cardiomyocyte proliferation was caused by apoptosis. The results showed that with the increase in the duration of hypoxia, caspase-3 activity gradually increased. In addition, NRF-1 overexpression could alleviate the high levels of caspase-3 activity. After NRF-1 was inhibited, caspase-3 activation became more pronounced. Subsequently, the real-time dynamic observation of cell growth showed that with the increase in caspase-3 activity, the nuclear red fluorescence became more evident. As the severity of nuclear membrane damage increased, nuclear condensation increased as well. However,

this process. These results further indicate that hypoxia-

induced damage caused to cardiomyocytes is partly triggered by apoptosis, and since NRF-1 can alleviate apoptosis, it can prevent the damage caused to cardiomyocytes under hypoxia.

Previous studies on NRF-1 have primarily focused on its effect on mitochondrial function and showed that NRF-1 could regulate the expression of mitochondrial respiratory chain complex gene family members, affecting mitochondrial biogenesis, and increase mitochondrial ATP production [47, 48]. Reportedly, NRF-1 can significantly improve the mitochondrial membrane potential in cardiomyocytes under hypoxia and enhance the mitochondrial respiratory capacity to increase cardiomyocyte viability [5]. Therefore, the anti-apoptotic effect of NRF-1 may be achieved by regulating apoptosis-related proteins associated with the mitochondria. Most of these molecules belong to the BCL-2 family, including some pro-apoptotic molecules, such as Bax, Bak, and Bid, and anti-apoptotic molecules, including BCL-2 and BCL-xL. At high levels, Bax can form dimers with other pro-apoptotic molecules, such as Bak and Bad, and form pore channels in the mitochondrial membrane, which results in cytochrome c release and a change in the mitochondrial membrane potential, eventually triggering apoptosis. BCL-2 and BCL-xL can competitively bind to Bax to reverse the effects of Bax binding to other apoptotic triggers, which helps achieve an anti-apoptotic effect. The interaction between anti-apoptotic and pro-apoptotic proteins of the BCL-2 family can directly determine the fate of different cardiac pathological processes, including myocardial infarction, dilated cardiomyopathy, and ischemic heart disease [49]. For example, BCL-2 can significantly reduce the infarct size caused by apoptosis [16, 50], whereas BCL-xL can inhibit the expression of the pro-apoptotic molecules Bax and Bid through different mechanisms [51]. Our results showed that decreased NRF-1 expression caused the expression of the anti-apoptotic molecules BCL-2 and BCL-xL to also decrease, while that of the pro-apoptotic molecule Bax was not affected. Since NRF-1 expression can be upregulated via human intervention, this increase can induce subsequent upregulation of BCL-2 and BCL-xL expression, thereby preventing or delaying their downregulation induced by hypoxia. Although the level of Bax did not increase significantly with hypoxia, NRF-1 could inhibit its expression. The above results indicate that the anti-apoptotic effect of NRF-1 on cardiomyocytes under hypoxia is achieved by promoting the expression of BCL-2/BCL-xL and inhibiting Bax expression.

These results indicate that NRF-1 exerts an anti-apoptotic effect in hypoxia-induced cardiomyocyte injury. The specific mechanism or the molecular control method adopted by NRF-1 for regulating the process remains to be studied. The central element in hypoxia is the reduction in oxygen concentration. The study of specific genes related to oxidative stress and the regulation of cardiomyocyte apoptosis by proteins encoded by these genes may help understand the regulatory mechanism. As mentioned above, proteins of the HIF family are extremely sensitive to oxygen. Under normoxia, they are degraded by proteases, while they remain stable under hypoxia. Among them, HIF-1 (HIF-1α and HIF-1β) is the most extensively studied molecule. It can affect apoptosis under hypoxia and in cardiac diseases in various ways [52, 53]. Firstly, we assessed whether NRF-1 targets HIF-1α. Transcription factors generally modulate molecular regulation by controlling the transcription levels of genes. The results showed that NRF-1 could inhibit *Hif1a* mRNA expression and led us to determine whether the effect is directly inhibited by binding or mediated by other regulatory processes. As mentioned above, NRF-1 exhibits a competitive relationship

found that NRF-1 could promote the expression of DNMT-1

[35] to maintain the level of methylation and further regulate spermatogenesis [13]. Besides maintaining methylation levels, DNMT-1 initiates methylation [52, 54]. Since NRF-1 inhibits the expression of HIF-1α, we attempted to evaluate the effect of the increase in methylation levels caused by methyltransferase-1 on the above relationship. The results showed that NRF-1 could bind to the promoter region of *Dnmt1* and regulate its expression, consistent with previous findings [13]. Subsequent studies showed that DNMT-1 expression decreases under prolonged hypoxia, whereas NRF-1 overexpression delayed this decline. Notably, according to an existing prediction website (http://alggen.lsi.upc.es/cgi-bin/promo_v3/promo/promoinit.cgi?dirDB=TF_8.3) and the contributions of previous reports [13], an NRF-1-binding sequence is found in human and mouse *Dnmt1*. Our analysis revealed that the same sequence also exists in rats, which indicates the conservation of the binding sequence and highlights the important regulatory role of NRF-1 in DNMT-1 expression. However, subsequent experiments showed that even though the promoter region of *Hif1a* predictably possessed a methylation site, there was no significant change in the methylation status before and after hypoxia, as shown by bisulfite sequencing PCR. Possibly, methylation is not the primary regulatory event affecting HIF-1α expression. Based on the above results, we conclude that NRF-1 negatively regulates HIF-1α expression by directly binding to the promoter region of *Hif1a*.

Previous studies have shown that HIF-1α acts as a protective molecule in cardiomyocytes under stress [55, 56]. It enhances cardiac tolerance to hypoxia in various ways, for instance, by enhancing anaerobic respiration and nucleotide metabolism and reducing cellular oxidative stress [57–60]. However, reportedly, HIF-1α can induce apoptosis, increase the myocardial infarct area, and promote damage [61, 62]. Therefore, the effect of HIF-1α on the heart has yet to be completely deciphered. To confirm the effect of HIF-1α on the apoptosis of rat cardiomyocytes under hypoxia, we performed the relevant experimental studies. The results showed that HIF-1α inhibition reduced cardiomyocyte proliferation under normoxia; however, following hypoxia, the proliferation of cardiomyocytes in the HIF-1α inhibition group decreased more significantly, and caspase-3 activity increased. These results indicate that HIF-1α exerts a protective effect on cardiomyocytes under hypoxia. To elucidate the negative regulatory effect of NRF-1 on HIF-1α and the effect of NRF-1 on cardiomyocyte apoptosis, we specifically inhibited NRF-1 expression in coordination with HIF-1α inhibition. Our data showed that under normoxia, the inhibition of both molecules reduced cardiomyocyte proliferation; however, compared with that in the HIF-1α inhibition group, the reduction in cardiomyocyte proliferation level was alleviated in the NRF-1 inhibition group, and caspase-3 activity was suppressed. Further analysis showed that HIF-1α inhibition increased the expression of the anti-apoptotic molecules BCL-2 and BCL-xL, and the levels of BCL-2/BCL-xL were relatively lower in the NRF-1 and HIF-1α inhibition group than in the HIF-1α inhibition group. Interestingly, HIF-1α inhibition led to an increase in NRF-1 expression, which has not been previously reported. This novel finding could also explain the simultaneous increase in BCL-2/BCL-xL expression with HIF-1α and NRF-1 inhibition. Superficially, HIF-1α inhibition leads to cardiomyocyte injury and apoptosis under hypoxia, which indicates that HIF-1α serves as an anti-apoptotic molecule under hypoxia. However, under the simultaneous inhibition of NRF-1, the cell morphology appeared qualitatively better than that in the HIF-1α inhibition group; this may be related to the fact that NRF-1 inhibition can partially restore HIF-1α

levels and alleviate, to a certain extent, cardiomyocyte hypoxia-induced injury. The results are concordant with the protective effect of HIF-1α on cardiomyocytes previously reported and suggest that HIF-1α plays a more significant anti-apoptotic role than NRF-1. The specific inhibition of HIF-1α expression was accompanied by an increase in BCL-2/BCL-xL expression, whereas after the simultaneous inhibition of NRF-1, BCL-2/BCL-xL expression decreased with a relative increase in HIF-1α expression; these findings were consistent with those reported previously by Choi et al. [63], Menrad et al. [64], and Zhao et al. [62], and indicated that BCL-2/BCL-xL is primarily affected by NRF-1 rather than by HIF-1α. The above results suggest that apoptosis caused by NRF-1-mediated inhibition of HIF-1α may not involve BCL-2 family proteins but by hitherto unknown mechanisms.

Since NRF-1 and HIF-1α exert the same anti-apoptotic effect, it is worth investigating why they exhibit mutual inhibition. It remains unknown whether the mutual inhibition is associated with the similar anti-apoptotic effects and the antagonism between the two molecules. HIF-1α regulates downstream genes by forming a dimer with HIF-1β. It has yet to be determined whether NRF-1 is involved in the formation of this dimer. However, our results indicated that NRF-1 could also bind to HIF-1β, and the binding levels gradually decrease under prolonged hypoxia, which reciprocally affects the binding with HIF-1α. In addition, the inhibition of NRF-1 expression led to an increase in the combination of HIF-1α and HIF-1β, suggesting a possible competitive binding between HIF-1α and HIF-1β. We used DMOG and BAY 87-2243 to verify our hypothesis and found that these two drugs did not affect HIF-1β expression and could positively or negatively regulate HIF-1α expression, respectively. The results showed that DMOG promoted HIF-1α expression, inhibited NRF-1 expression, and suppressed the binding between NRF-1 and HIF-1β. However, when BAY 87-2243 was used to inhibit HIF-1α, a contrasting yet consistent phenomenon was observed—HIF-1α inhibition increased NRF-1 expression, as well as increased the binding levels of NRF-1 and HIF-1β. This phenomenon may be related to the adaptation of cells to hypoxic stress. The above results indicate that under normal conditions, NRF-1 acts as a key transcription factor that exerts multiple effects on cardiomyocyte molecular regulation. In the absence of external stimulation, NRF-1 and other nuclear molecules, including HIF-1β, form a key complex and participate in the regulation of mitochondrial function, cell growth, and metabolism. However, under prolonged hypoxia, the expression of NRF-1 decreases gradually, which leads to the loss of cell function. As an adaptation to hypoxia and to promote survival, HIF-1α accumulates, gradually replacing NRF-1, which promotes the binding between HIF-1α and HIF-1β. Certain key molecules, such as CD39, CD73, p53, and LDHA, are expressed, facilitating cell tolerance to hypoxia. This could explain why HIF-1α can promote hypoxia tolerance in cardiomyocytes and aggravate cardiomyocyte injury under different hypoxic conditions [65, 66]. The exact reason for aggravation of cardiomyocyte injury still needs to be investigated.

Lastly, we examined the role of PGC-1α. Several studies have indicated the involvement of PGC-1α in processes related to apoptosis regulation, such as p53 gene-mediated apoptosis, enhancement of mitochondrial recovery to reduce apoptosis, and regulation of the expression of apoptosis-related molecules [67–69]. Results showed that PGC-1α levels gradually decreased with the increase of hypoxia duration, and this change was not affected by NRF-1 inhibition, indicating that PGC-1α is a transcription

ding was consistent with previous reports [70–71]. Our

results also showed that NRF-1 and PGC-1α could form stable dimers, and the binding levels of NRF-1 and PGC-1α did not change as the duration of hypoxia was prolonged. Next, upon stimulating the cells with DMOG, the same effect observed for NRF-1 was observed. When PGC-1α expression was promoted upon ZLN005 treatment, the levels of NRF-1 and PGC-1α increased and the levels of NRF-1 and HIF-1β binding increased during the initial stages of hypoxia (0 and 6 h), whereas the binding between HIF-1α and HIF-1β was suppressed. However, the enhanced binding effect was gradually reversed by HIF-1α because the levels of the two molecules decreased with the increase in the duration of hypoxia. These results suggest that PGC-1α, as an upstream transcription regulator of NRF-1, is also involved in regulating the competitive binding between NRF-1 and HIF-1α. However, whether PGC-1α directly binds to HIF-1α or indirectly binds to HIF-1β by binding with NRF-1 needs to be studied further.

Conclusion

Our results indicate that NRF-1 can alleviate cardiomyocyte apoptosis and improve cardiomyocyte viability under hypoxia. Moreover, HIF-1α serves as an important anti-apoptotic molecule under hypoxia. To the best of our knowledge, this is the first study to report that NRF-1 cooperatively acts with PGC-1α and competes with HIF-1α to bind HIF-1β. This molecular regulatory process may be related to cardiomyocyte adaptation to hypoxia and may promote cell survival under low-oxygen stress. This study provides a novel theoretical framework for improving the protection mechanisms for hypoxia-induced myocardial injury; however, the specific molecular process warrants further investigation.

List Of Abbreviations

DMEM Dulbecco's modified Eagle's medium

FBS Fetal bovine serum

HIF Hypoxia-inducible factors

PCR Polymerase chain reaction

Declarations

Acknowledgments

The authors thank the members of the Institute of Medical Sciences of Ningxia Hui Autonomous Region for providing excellent technical assistance.

Competing interests

The authors declare no competing interests.

Funding

This work was supported by the Natural Science Foundation of Ningxia Hui Autonomous Region, HL was the project leader [grant number 2020AAC03425].

Data availability

All data related to this study are available from the corresponding author upon reasonable request

Ethics approval and consent to participate

Not Applicable.

Consent for publication

Not applicable.

Authors' contributions

Nan Niu and Wei Zhao designed and revised the experiment. Nan Niu wrote the manuscript. Nan Niu, Hui Li, Xiancai Du and Junliang Li performed main experiment, Jihui Yang and Cheng Liu performed the cell sorting. Chan Wang, Songhao Yang performed the packaging of the virus. Chan Wang and Yazhou Zhu performed the cell images.

References

1. Rustamova Y , Lombardi M . Ischemic Heart Disease. Cardiac Magnetic Resonance Atlas. 2020.
2. Savla JJ, Levine BD, Sadek, HA. The effect of hypoxia on cardiovascular disease: friend or foe? High Alt Med Biol. 2018;19:124-30.
3. Virzì GM, Clementi A, Ronco C. Cellular apoptosis in the cardiorenal axis. Heart Fail Rev. 2016;21:177-89.
4. Xuan Y, Liu S, Li Y, Dong J, Luo J, Liu T, et al. Shortterm vagus nerve stimulation reduces myocardial apoptosis by downregulating microRNA205 in rats with chronic heart failure. Mol Med Rep. 2017;16:5847-54.
5. Niu N, Li Z, Zhu M, Sun H, Yang J, Xu S, et al. Effects of nuclear respiratory factor-1 on apoptosis and mitochondrial dysfunction induced by cobalt chloride in H9C2 cells. Mol Med Rep. 2019;19:2153-63.
6. Gopalakrishnan L, Scarpulla RC. Structure, expression, and chromosomal assignment of the human gene encoding nuclear respiratory factor 1. J Biol Chem. 1995;270:18019-25.
7. Chau CM, Evans MJ, Scarpulla RC. Nuclear respiratory factor 1 activation sites in genes encoding the gamma-subunit of ATP synthase, eukaryotic initiation factor 2 alpha, and tyrosine aminotransferase. Specific interaction of purified NRF-1 with multiple target genes. J Biol Chem. 1992;267:6999-7006.
8. Gao W, Wu M, Wang N, Zhang Y, Wang Y. Increased expression of mitochondrial transcription factor A and nuclear respiratory factor-1 predicts a poor clinical outcome of breast cancer. Oncol Lett.

9. Suliman HB, Sweeney TE, Withers CM, Piantadosi, CA. Co-regulation of nuclear respiratory factor-1 by NFkappaB and CREB links LPS-induced inflammation to mitochondrial biogenesis. J Cell Sci. 2010;123:2565-75.
10. Remels AH, Pansters NA, Gosker HR, Schols AM, Langen RC. Activation of alternative NF-κB signaling during recovery of disuse-induced loss of muscle oxidative phenotype. Am J Physiol Endocrinol Metab. 2014;306:E615-26.
11. Morrish F, Giedt C, Hockenbery D. c-MYC apoptotic function is mediated by NRF-1 target genes. Genes Dev. 2003;17:240-55.
12. Radde BN, Ivanova MM, Mai HX, Alizadeh-Rad N, Piell K, Van Hoose P, et al. Nuclear respiratory factor-1 and bioenergetics in tamoxifen-resistant breast cancer cells. Exp Cell Res. 2016;347:222-31.
13. Wang J, Tang C, Wang Q, Su J, Ni T, Yang W, et al. NRF1 coordinates with DNA methylation to regulate spermatogenesis. FASEB J. 2017;31:4959-70.
14. Claude AP. Heme oxygenase-1 regulates cardiac mitochondrial biogenesis via Nrf2-mediated transcriptional control of nuclear respiratory factor-1. Circ Res. 2008;103:1232-40.
15. Dangsheng L. PGC-1alpha: looking behind the sweet treat for porphyria. Cell 2005;122:487-9.
16. Chen SD, Yang DI, Lin TK, Shaw FZ, Liou CW, Chuang YC. Roles of oxidative stress, apoptosis, PGC-1α and mitochondrial biogenesis in cerebral ischemia. Int J Mol Sci. 2011;12:7199-215.
17. Cheng CF, Ku HC, Lin H. PGC-1α as a pivotal factor in lipid and metabolic regulation. Int J Mol Sci. 2018;19:3447.
18. Chiu KC, Tse PW, Law CT, Xu MJ, Wong CL. Hypoxia regulates the mitochondrial activity of hepatocellular carcinoma cells through HIF/HEY1/PINK1 pathway. Cell Death Dis. 2019;10:934.
19. Li HS, Zhou YN, Li L, Li SF, Long D, Chen XL, et al. (2019). HIF-1α protects against oxidative stress by directly targeting mitochondria. Redox Biol. 2019;25:101109.
20. Varghese, R., Sridharan, S., Datta, A. and Venkatraj, J. Modeling hypoxia stress response pathways. In IEEE International Workshop on Genomic Signal Processing & Statistics. 2013. DOI: 10.1109/GENSIPS.2013.6735939
21. Semenza GL. Hypoxia-inducible factors in physiology and medicine. Cell 2012;148:399-408.
22. Jain T, Nikolopoulou EA, Xu Q, Qu A. Hypoxia inducible factor as a therapeutic target for atherosclerosis. Pharmacol Ther. 2018;183:22-33.
23. Ke-Yuan S, Gao-Zhong H, Fang Y, Shi-Hong C, Guo-Xiang FU, Geriatrics DO, et al. Value of hypoxia-inducible factor 1α in diagnosis and prognosis of acute decompensated chronic heart failure. journal of shanghai jiaotong university (medical science). 2018
24. Meng X, Grötsch B, Luo Y, Knaup KX, Wiesener MS, Chen XX, et al. Hypoxia-inducible factor-1α is a critical transcription factor for IL-10-producing B cells in autoimmune disease. Nat Commun. 2018;9:251.
25. Gao Y, Yin H, Zhang Y, Dong Y, Yang F, Wu X, et al. Dexmedetomidine protects hippocampal neurons against hypoxia/reoxygenation-induced apoptosis through activation HIF-1α/p53 signaling. Life Sci.

2019;232:116611.
26. Guo Y. Role of HIF-1a in regulating autophagic cell survival during cerebral ischemia reperfusion in rats. Oncotarget 2017;8:98482-94.
27. Trisciuoglio D, Gabellini C, Desideri M, Ziparo E, Zupi G, Del Bufalo D. Bcl-2 regulates HIF-1a protein stabilization in hypoxic melanoma cells via the molecular chaperone HSP90. PLoS One. 2010;5:e11772.
28. Wei J, Wu J, Xu W, Nie H, Zhou R, Wang R, et al. Salvanic acid B inhibits glycolysis in oral squamous cell carcinoma via targeting PI3K/AKT/HIF-1α signaling pathway. Cell Death Dis. 2018;9:599.
29. Li LC. Chromatin remodeling by the small RNA machinery in mammalian cells. Epigenetics. 2014;9:45-52.
30. Portoy V, Lin SHS, Li KH, Burlingame A, Hu ZH, Li H, et al. saRNA-guided Ago2 targets the RITA complex to promoters to stimulate transcription. Cell Res. 2016;26:320-35.
31. Wang J, Place RF, Portnoy V, Huang V, Kang MR, Kosaka M, et al. Inducing gene expression by targeting promoter sequences using small activating RNAs. J Biol Methods. 2011;2:e14.
32. Khalilzadeh B, Shadjou N, Kanberoglu GS, Afsharan H, de la Guardia M, Charoudeh HN, et al. Advances in nanomaterial based optical biosensing and bioimaging of apoptosis via caspase-3 activity: a review. Mikrochim Acta. 2018;185:434.
33. Kim R, Emi M, Tanabe K. Caspase-dependent and -independent cell death pathways after DNA damage (Review). Oncol Rep. 2005;14:595-9.
34. Wang D, Zhang J, Lu Y, Luo Q, Zhu L. Nuclear respiratory factor-1 (NRF-1) regulated hypoxia-inducible factor-1α (HIF-1α) under hypoxia in HEK293T. IUBMB Life. 2016;68:748-55.
35. Domcke S, Bardet AF, Ginno PA, Hartl D, Burger L, Schübeler D. Competition between DNA methylation and transcription factors determines binding of NRF1. Nature 2015;528:575-9.
36. Baader E, Tschank G, Baringhaus KH, Burghard H, Günzler V. Inhibition of prolyl 4-hydroxylase by oxalyl amino acid derivatives in vitro, in isolated microsomes and in embryonic chicken tissues. Biochem J. 1994;300:525-30.
37. Schultz K, Murthy V, Tatro JB, Beasley D. Prolyl hydroxylase 2 deficiency limits proliferation of vascular smooth muscle cells by hypoxia-inducible factor-1α-dependent mechanisms. Am J Physiol Lung Cell Mol Physiol. 2009;296:L921-7.
38. Xia P, Liu Y, Cheng Z. Signaling pathways in cardiac myocyte apoptosis. Biomed Res Int. 2016;2016:9583268.
39. Gill C, Mestril R, Samali A. Losing heart: the role of apoptosis in heart disease—a novel therapeutic target? FASEB J. 2002;16:135-46.
40. Narula J, Kolodgie FD, Virmani R. Apoptosis and cardiomyopathy. Curr Opin Cardiol. 2000;15:183.
41. Polunina OS, Voronina LP, Mukhambetova GN, Maslyaeva GY, Voronina PN. Analysis of level of apoptosis markers in patients with coronary heart disease. Medical Alphabet 2020;4:5-8
42. Toringova E, Tousek PA. Apoptosis in ischemic heart disease. J Transl Med. 2017;15:87.

43. Huo L, Scarpulla RC. Mitochondrial DNA instability and peri-implantation lethality associated with targeted disruption of nuclear respiratory factor 1 in mice. Mol Cell Biol. 2001;21:6449-54.
44. Condorelli G, Roncarati R, Ross J Jr, Pisani A, Stassi G, Todaro M, et al. Heart-targeted overexpression of caspase3 in mice increases infarct size and depresses cardiac function. Proc Natl Acad Sci U S A. 2001;98:9977-82.
45. Liu H, Liu S, Tian X, Wang Q, Rao J, Wang Y, et al. Bexarotene attenuates focal cerebral ischemia-reperfusion injury via the suppression of JNK/Caspase-3 signaling pathway. Neurochem Res. 2019;44:2809-20.
46. Liu Q. Lentivirus mediated interference of Caspase-3 expression ameliorates the heart function on rats with acute myocardial infarction. Eur Rev Med Pharmacol Sci. 2014;18:1852-8.
47. Hsieh PF, Liu SF, Hung TJ, Hung CY, Liu GZ, Chuang LY, et al. Elucidation of the therapeutic role of mitochondrial biogenesis transducers NRF-1 in the regulation of renal fibrosis. Exp Cell Res. 2016;349:23-31.
48. Napolitano G, Barone D, Di Meo S, Venditti P. Adrenaline induces mitochondrial biogenesis in rat liver. J Bioenerg Biomembr. 2018;50:11-9.
49. Gustafsson AB, Gottlieb RA. Bcl-2 family members and apoptosis, taken to heart. Am J Physiol Cell Physiol. 2007;292:C45-51.
50. Brocheriou V, Hagège AA, Oubenaïssa A, Lambert M, Mallet VO, Duriez M, et al. Cardiac functional improvement by a human Bcl-2 transgene in a mouse model of ischemia/reperfusion injury. Gene Med. 2000;2:326-33.
51. Garcia A, Murad F. Bcl-xL inhibits tBid and Bax via distinct mechanisms. Faraday Discuss, in press. 2020. doi: 10.1039/D0FD00045K
52. Li Y, Zhang Z, Chen J, Liu W, Lai W, Liu B, et al. Stella safeguards the oocyte methylome by preventing de novo methylation mediated by DNMT1. Nature. 2018;564:136-40.
53. Yin J, Ni B, Liao WG, Gao YQ. Hypoxia-induced apoptosis of mouse spermatocytes is mediated by HIF-1α through a death receptor pathway and a mitochondrial pathway. J Cell Physiol. 2018;233:1146-55.
54. Svedružić ŽM. Dnmt1 structure and function. Prog Mol Biol Transl Sci. 2011;101:221-54.
55. de Castro AL, Fernandes RO, Ortiz VD, Campos C, Bonetto JHP, Fernandes TRG, et al. Cardioprotective doses of thyroid hormones improve NO bioavailability in erythrocytes and increase HIF-1α expression in the heart of infarcted rats. Arch Physiol Biochem, in press. 2020. doi: 10.1080/13813455.2020.1779752
56. Nanayakkara G, Alasmari A, Mouli S, Eldoumani H, Quindry J, McGinnis G, et al. Cardioprotective HIF-1α-frataxin signaling against ischemia-reperfusion injury. Am J Physiol Heart Circ Physiol. 2015;309:H867-79.
57. Lin F, Pan LH, Ruan L, Qian W, Liang R, Ge WY, et al. Differential expression of HIF-1α, AQP-1, and VEGF under acute hypoxic conditions in the non-ventilated lung of a one-lung ventilation rat model.

58. Ong SG, Lee WH, Theodorou L, Kodo K, Lim SY, Shukla DH, et al. HIF-1 reduces ischaemia-reperfusion injury in the heart by targeting the mitochondrial permeability transition pore. Cardiovasc Res. 2014;104:24-36.
59. Reischl S, Li L, Walkinshaw G, Flippin LA, Marti HH, Kunze R. Inhibition of HIF prolyl-4-hydroxylases by FG-4497 reduces brain tissue injury and edema formation during ischemic stroke. PLoS One. 2014;9:e84767.
60. Wu J, Bond C, Chen P, Chen M, Li Y, Shohet RV, et al. HIF-1α in the heart: remodeling nucleotide metabolism. J Mol Cell Cardiol. 2015;82:194-200.
61. Chen YF, Pandey S, Day CH, Chen YF, Jiang AZ, Ho TJ, et al. Synergistic effect of HIF-1α and FoxO3a trigger cardiomyocyte apoptosis under hyperglycemic ischemia condition. J Cell Physiol. 2018;233:3660-71.
62. Zhao X, Liu L, Li R, Wei X, Luan W, Liu P, et al. Hypoxia-Inducible Factor 1-α (HIF-1α) induces apoptosis of human uterosacral ligament fibroblasts through the death receptor and mitochondrial pathways. Med Sci Monit. 2018;24:8722-33.
63. Choi SC, Ho YF, Tsang WP, Kwok TT. The roles of HIF-1α and p53 in severe hypoxia induced apoptosis. Cancer Res. 2008;68:1820.
64. Menrad H, Werno C, Schmid T, Copanaki E, Deller T, Dehne N, et al. Roles of hypoxia-inducible factor-1alpha (HIF-1alpha) versus HIF-2alpha in the survival of hepatocellular tumor spheroids. Hepatology 2010;51:2183-92.
65. Yang J, He F, Meng Q, Sun Y, Wang W, Wang C. Inhibiting HIF-1α decreases expression of TNF-α and Caspase-3 in specific brain regions exposed kainic acid-induced status epilepticus. Cell Physiol Biochem. 2016;38:75-82.
66. Yeh YL, Hu WS, Ting WJ, Shen CY, Hsu HH, Chung LC, et al. Hypoxia augments increased HIF-1α and reduced survival protein p-Akt in Gelsolin (GSN)-dependent cardiomyoblast cell apoptosis. Cell Biochem Biophys. 2016;74:221-8.
67. Intihar TA, Martinez EA, Gomez-Pastor R. Mitochondrial dysfunction in Huntington's disease; interplay between HSF1, p53 and PGC-1α transcription factors. Front Cell Neurosci. 2019;13:103.
68. Nasehi M, Torabinejad S, Hashemi M, Vaseghi S, Zarrindast MR. Effect of cholestasis and NeuroAid treatment on the expression of Bax, Bcl-2, Pgc-1α and Tfam genes involved in apoptosis and mitochondrial biogenesis in the striatum of male rats. Metab Brain Dis. 2020;35:183-92.
69. Zhang Q, Liang XC. Effects of mitochondrial dysfunction via AMPK/PGC-1α signal pathway on pathogenic mechanism of diabetic peripheral neuropathy and the protective effects of Chinese medicine. Chin J Integr Med. 2019;25:386-94.
70. Bremer K, Kocha KM, Snider T, Moyes CD. Sensing and responding to energetic stress: The role of the AMPK-PGC1α-NRF1 axis in control of mitochondrial biogenesis in fish. Comp Biochem Physiol B Biochem Mol Biol. 2016;199:4-12.
71. Chong H, Wei Z, Na M, Sun G, Zheng S, Zhu X, et al. The PGC-1α/NRF1/miR-378a axis protects -induced proliferation, migration and inflammation in

atherosclerosis. Atherosclerosis. 2002;297:136-45.

Figures

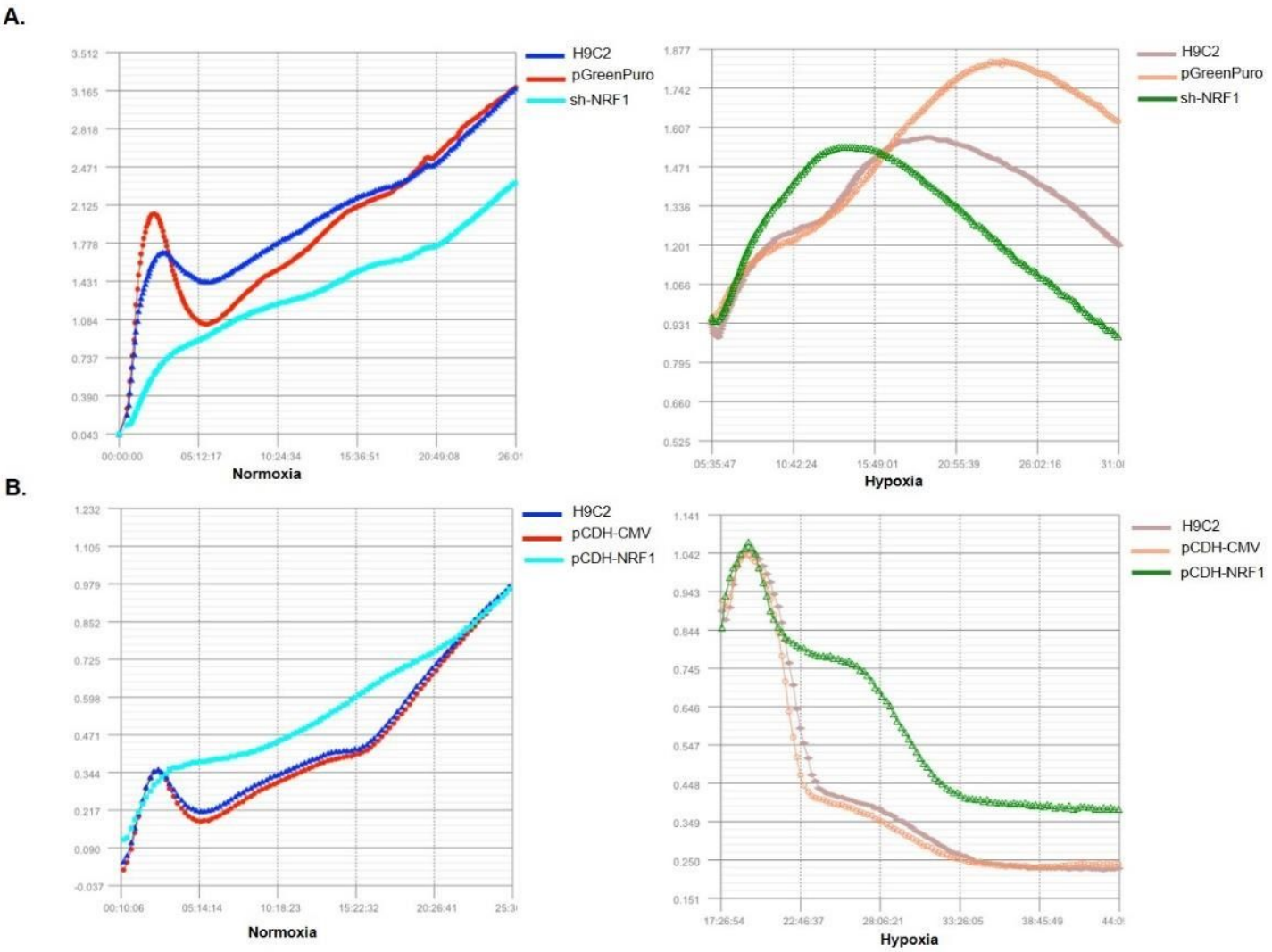

Figure 1

Evaluation of cell proliferation. Cardiomyocyte proliferation was monitored using an ACEA iCell real-time cell proliferation analyzer. Cell proliferation was monitored every 10 min for 24 h. A, B. Left, the proliferation of cardiomyocytes under normoxia; right, proliferation of cardiomyocytes under hypoxia (1% O2).

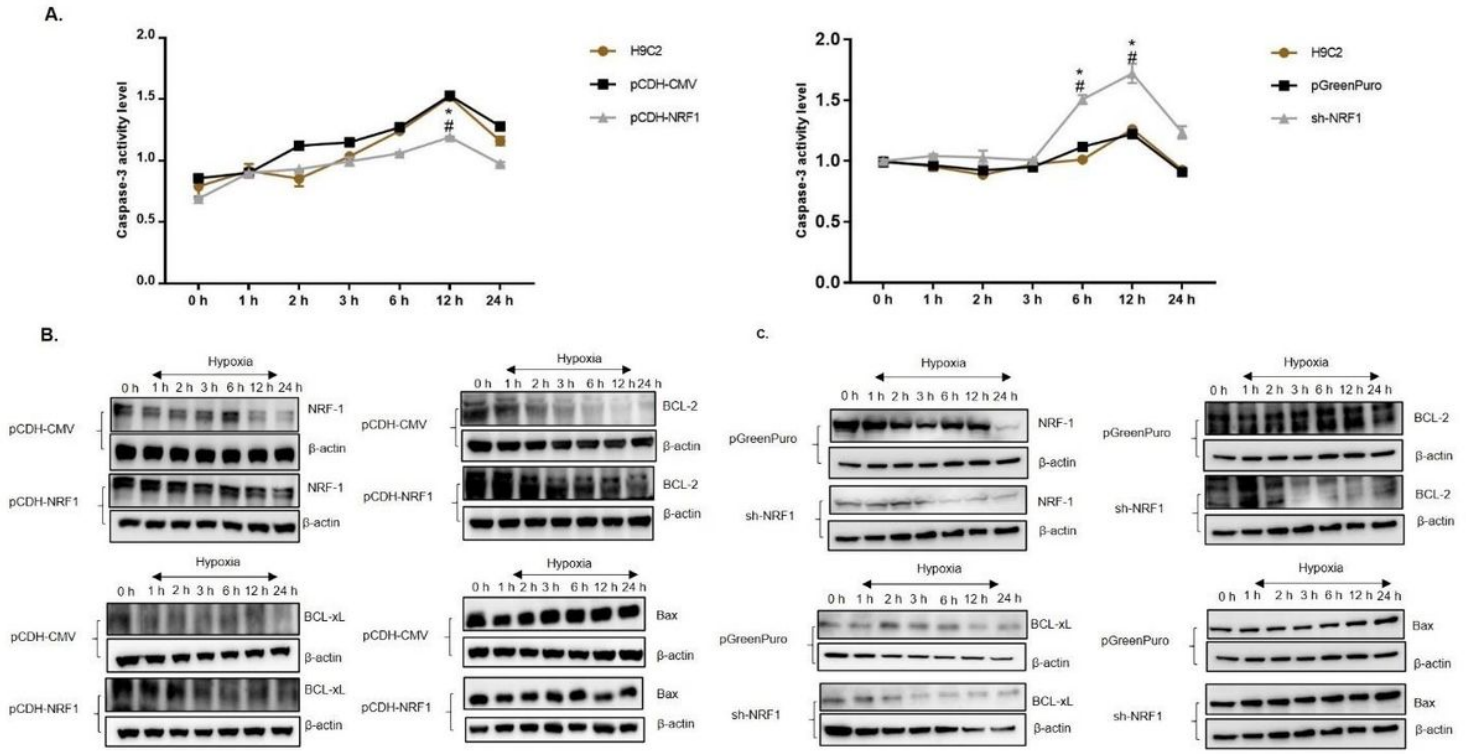

Figure 2

Assessment of cardiomyocyte apoptosis under hypoxia. A. Measurement of caspase-3 activity, *P < 0.05, vs. H9C2. #P < 0.05, vs. pCDH-CMV or pGreenPuro. B. Followed by the NRF-1 overexpression (pCDH-NRF1), compared to those in pCDH-CMV, the levels of NRF-1, BCL-2, BCL-xL, and Bax changed after the cells were subjected to hypoxia (at 1% O2) for 0, 1, 2, 3, 6, 12, and 24 h. C. Following NRF-1 inhibition (sh-NRF1), the levels of NRF-1, BCL-2, BCL-xL, and Bax changed after the cells were subjected to hypoxia (at 1% O2) for 0, 1, 2, 3, 6, 12, and 24 h. Bad: BCL-associated agonist of cell death; Bak: BCL-2 homologous antagonist/killer; Bax: BCL-2-associated X protein; BCL-2: B-cell lymphoma 2; BCL-xl: BCL-extra-large; NRF-1: nuclear respiratory factor-1.

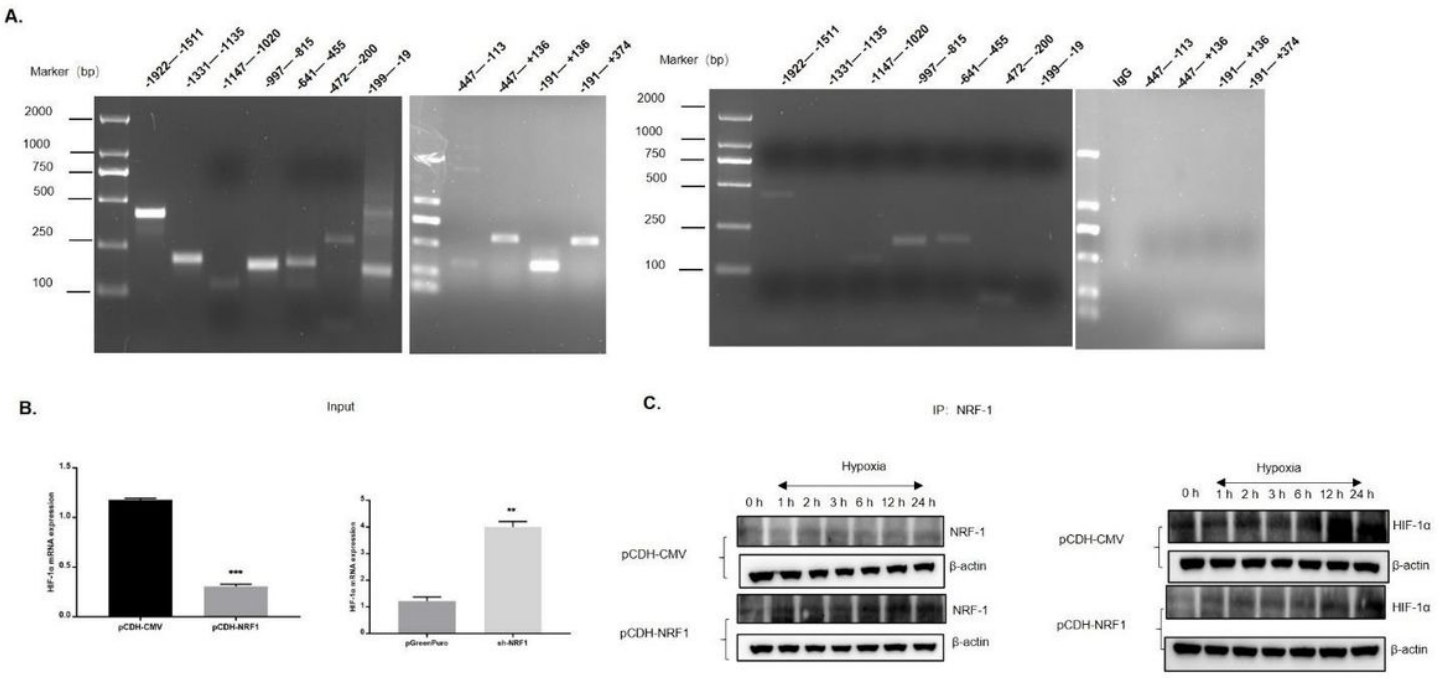

Figure 3

Effect of NRF-1 on HIF-1α expression. A. The binding level of NRF-1 to the binding element in the Hif1a promoter region was determined using ChIP. B. Effects of NRF-1 on Hif1a mRNA were assessed by a quantitative polymerase chain reaction. **P < 0.01, ***P < 0.01, vs. pCDH-CMV or pGreenPuro. Data are presented as mean ± standard deviation (n = 3). C. Western blotting was performed to ascertain the effect of NRF-1 on HIF-1α protein levels after the cells were subjected to hypoxia for 0, 1, 2, 3, 6, 12, and 24 h. ChIP: chromatin immunoprecipitation; HIF: hypoxia-inducible factor; NRF-1: nuclear respiratory factor-1; PGC-1α: peroxisome proliferator-activated receptor gamma coactivator 1-alpha.

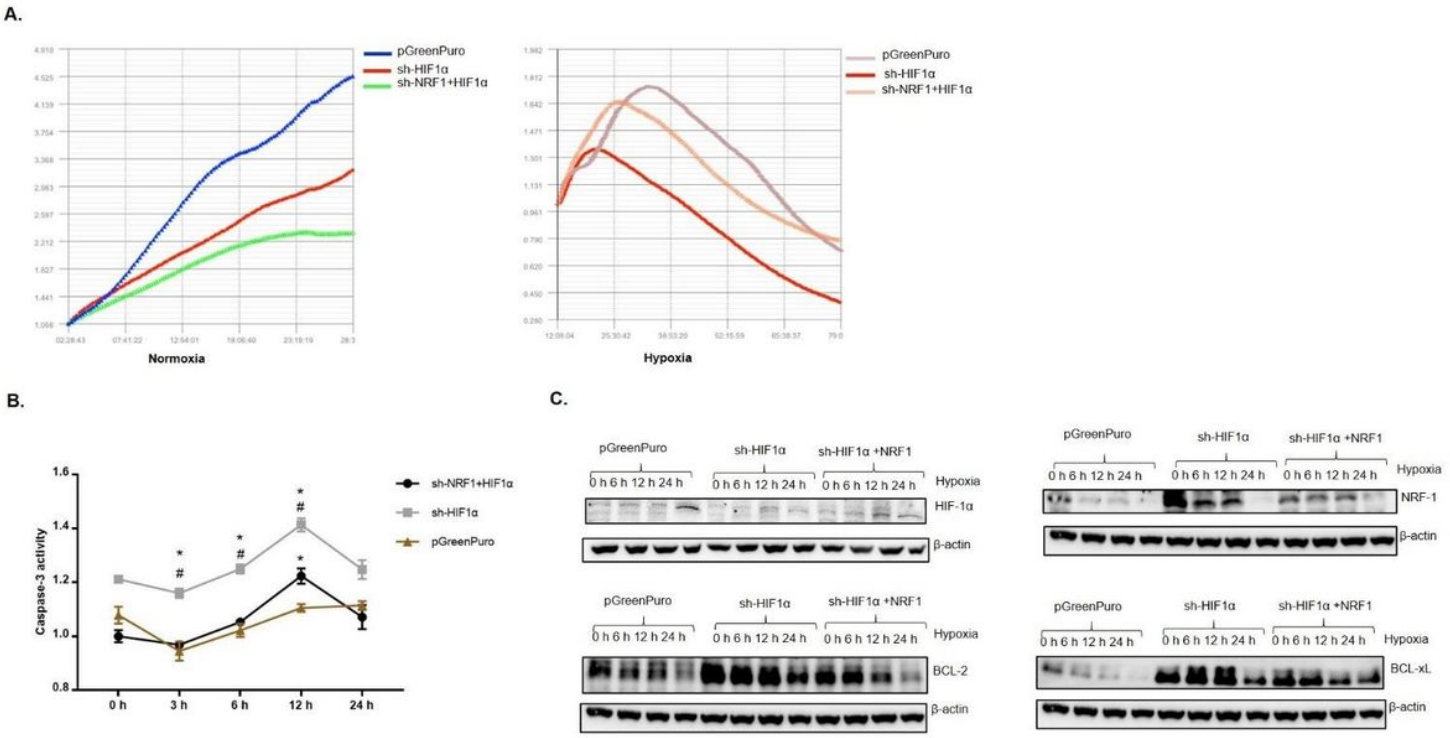

Figure 4

Effect of NRF-1 and HIF-1α on cardiomyocyte apoptosis. A. Evaluation of cardiomyocyte proliferation in each group. B. Caspase-3 activity under hypoxia. C. The levels of HIF-1α, NRF-1, BCL-2, and BCL-xL were determined by western blotting. *P < 0.05 vs. pGreenPuro. #P < 0.05 showed sh-HIF1α vs. sh-HIF1α+NRF1. BCL-2: B-cell lymphoma 2; BCL-xl: BCL-extra-large; HIF: hypoxia-inducible factor; NRF-1: nuclear respiratory factor-1.

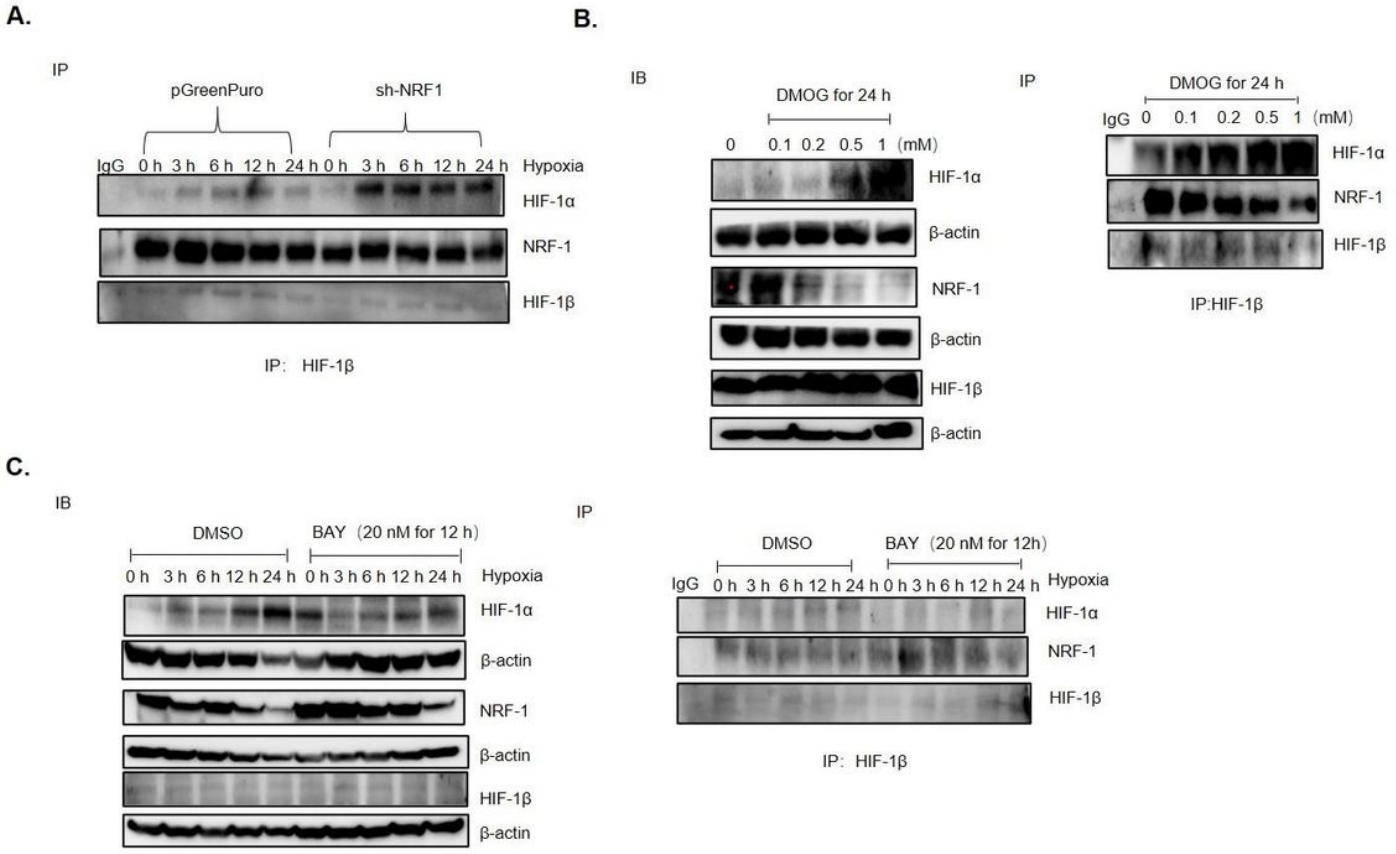

Figure 5

Immunoprecipitation for determination of the level of NRF-1, HIF-1α, and HIF-1β binding. A. The binding levels of NRF-1, HIF-1α, and HIF-1β were studied after the inhibition of NRF-1 (sh-NRF1) under hypoxia. B. After treatment with different DMOG concentrations (0, 0.1, 0.2, 0.5, and 1 mM), the expression and binding levels of NRF-1, HIF-1α, and HIF-1β in cardiomyocytes were observed. C. After treatment with 20 nM BAY 87-2243 for 12 h, the expression and binding levels of NRF-1, HIF-1α, and HIF-1β were observed under hypoxia for different durations. DMOG: dimethyloxallyl glycine; HIF: hypoxia-inducible factor; NRF-1: nuclear respiratory factor-1.

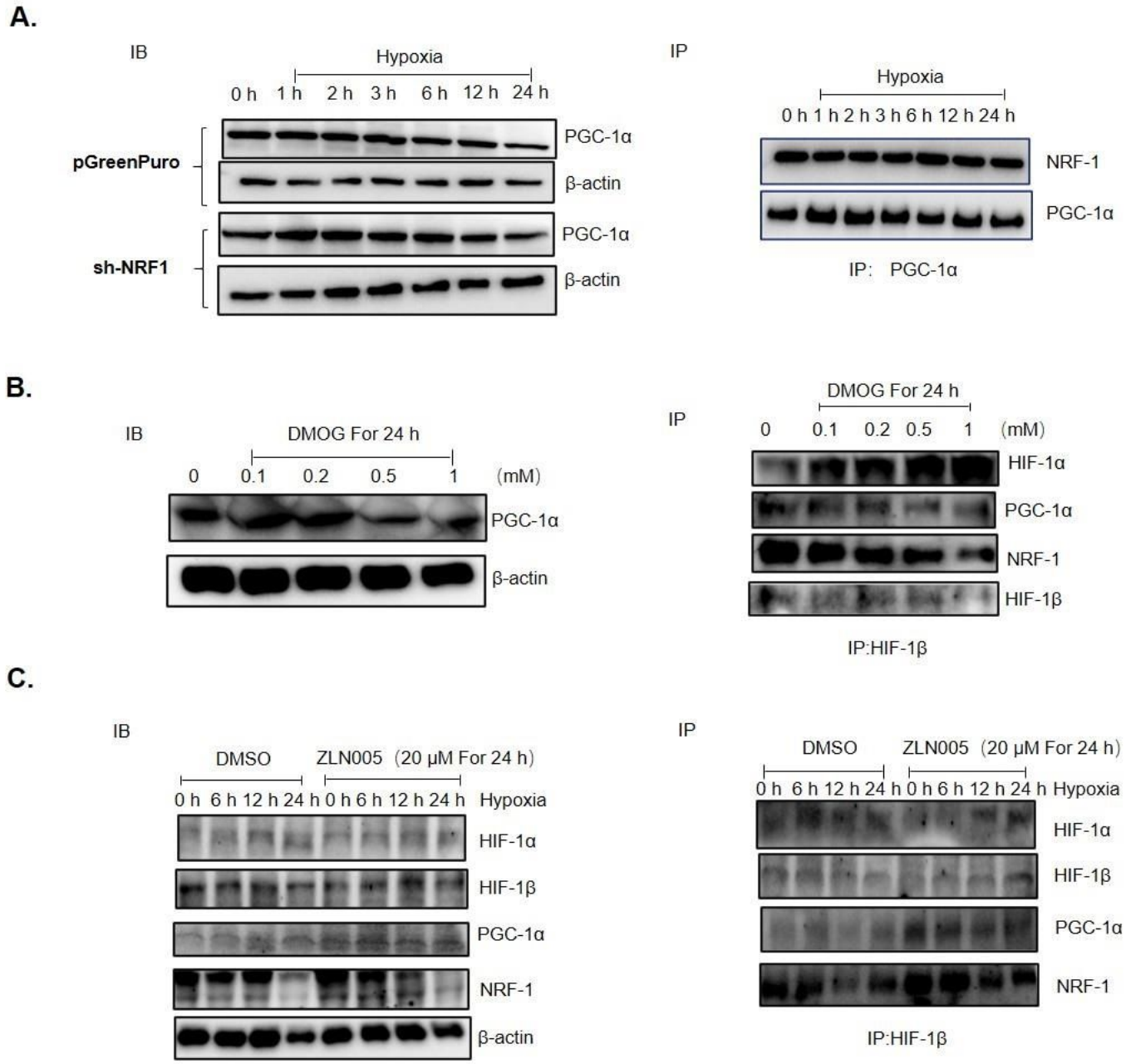

Figure 6

Role of PGC-1α in the competitive binding of HIF-1α and NRF-1 with HIF-1β. A. Left, levels of PGC-1α in each group; right, binding levels of PGC-1α and NRF-1 under hypoxia. B. Left, the effect of different concentrations of DMOG on PGC-1α; right, binding levels of HIF-1α, NRF-1, and PGC-1α with HIF-1β. C. Left, changes in the levels of HIF-1α, NRF-1, PGC-1α, and HIF-1β after treatment with ZLN005 for 24 h under hypoxia for 0, 6, 12, and 24 h; right, binding levels of HIF-1α, NRF-1, and PGC-1α with HIF-1β. DMOG: dimethyloxallyl glycine; HIF: hypoxia-inducible factor; NRF-1: nuclear respiratory factor-1; PGC-1α: peroxisome proliferator-activated receptor gamma coactivator 1-alpha.

Supplementary Files

This is a list of supplementary files associated with this preprint. Click to download.

- SupplementaryFigure.pdf
- Video58.rar
- Video14.rar